Prospective Sensitity to WIMP Dark Matter with the IceCube Upgrade

The IceCube Collaboration

(a complete list of authors can be found at the end of the proceedings)

E-mail: eliot.genton@uclouvain.be, jeffrey.lazar@uclouvain.be, carguelles@g.harvard.edu, gwenhael.dewasseige@uclouvain.be

While astrophysical observations imply that 85% of the matter content is unaccounted for, the nature of this dark matter (DM) component remains unknown. Weakly Interacting Massive Particles (WIMPs)—DM particles that interact at or below the weak interaction scale—could naturally explain this missing matter. These interactions with the Standard Model (SM) allow them to be gravitationally captured in celestial bodies like the Sun. Trapped DM in the solar core could subsequently annihilate, producing stable SM particles, of which only neutrinos can escape the Sun's dense interior. Therefore, an excess of neutrinos originating from the direction of the Sun would serve as evidence of DM. The IceCube Upgrade, a dense infill of the IceCube Neutrino Observatory, will lower the energy threshold and improve sensitivity in the range from 1 to 500 GeV, thereby enhancing IceCube's ability to detect GeV-scale DM. In this contribution, I present projections of the IceCube Upgrade's sensitivity to the DM-proton scattering cross section for DM masses between 3 GeV and 500 GeV. These sensitivities position IceCube as the most sensitive indirect detection experiment for DM in the mass range from 3 GeV to 10 TeV.
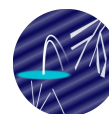
Corresponding authors: Jeffrey Lazar[1*], Eliot Genton[12*], Gwenhaël de Wasseige[1], Carlos Argüelles[2]

[1] *Center for Cosmology, Particle Physics and Phenomenology, UCLouvain*

[2] *Laboratory of Particle Physics and Cosmology, Harvard*

* Presenter

1. Introduction

Neutrinos originating from the Sun have historically provided key insights into both astrophysics and particle physics. Observations of low-energy solar neutrinos confirmed the Sun's energy production via nuclear fusion and revealed the phenomenon of neutrino oscillations, providing evidence for nonzero neutrino mass [1]. While solar neutrino studies at MeV energies are well established, the GeV-scale regime remains relatively unexplored and offers new potential for discovery.

Beyond the Standard Model (SM), high-energy neutrino fluxes may arise from the annihilation of dark matter (DM) accumulated in the solar core. Low-mass DM, a well-motivated DM candidate, could become gravitationally captured by the Sun following scatterings with solar nuclei. Over time, an excess of DM may accumulate and annihilate into Standard Model particles, among which only neutrinos can escape from the dense solar environment. These neutrinos offer a unique avenue for indirect detection of dark matter, complementary to terrestrial direct detection experiments [2].

2. The IceCube Upgrade

The IceCube Neutrino Observatory, a cubic-kilometer-scale neutrino telescope located at the geographic South Pole, is uniquely positioned to search for high-energy neutrinos from DM annihilation in the Sun [3]. It consists of 5,160 Digital Optical Modules (DOMs) deployed at depths between 1.450 m and 2.450 m along 86 vertical strings, to reduce the contamination from muons produced by the interactions of cosmic rays in the earths atmosphere. IceCube is designed primarily to detect high-energy neutrinos from astrophysical sources, with optimal sensitivity in the energy range from approximately 100 GeV to several PeV. Neutrinos are detected indirectly through the Cherenkov radiation emitted by charged secondary leptons, produced in neutrino interactions with the Antarctic ice, that traverse the detector at velocities exceeding the local speed of light. This Cherenkov light is captured by the DOMs, enabling the reconstruction of the energy, direction, and flavor of the incident neutrinos.

The DeepCore subarray, located in the central region of IceCube, features reduced vertical and horizontal spacing between DOMs, resulting in greater sensitivity to faint Cherenkov light and enabling IceCube to detect neutrinos with energies as low as $O(\text{GeV})$. This current configuration as of July 2025 is designated as "IC86". Looking ahead, the forthcoming IceCube Upgrade will reinforce DeepCore by introducing seven new strings equipped with advanced multi-PMT DOMs, thereby increasing the detector's DOM density and expanding its fiducial volume. This future IceCube Upgrade configuration, designated as "IC93", will push the energy threshold down to $O(1\text{GeV})$ and the multi-PMT structure of the added DOMs will also help substantially refine the reconstruction of neutrino direction and energy [4]. The layout structure of the different mentioned arrays is given in Fig. 1. Fig. 2a and Fig. 2b compare two key reconstruction parameters—angular resolution and effective area—for both IC86 and upgraded IceCube IC94 configurations. It should be noted that the sample used to construct the IC86 distributions, which was employed in previous IceCube solar dark matter analyses, was derived from a dataset originally optimized for oscillation studies rather than astronomy. This selection excludes events with light detected outside the DeepCore region, thereby suppressing higher energy events.

In IceCube, observed neutrino interactions are typically categorized according to their *dominant event topology*: either track-like or cascade-like (shower-like). Most events display a single topology, but some can exhibit both track and cascade features simultaneously, depending on the underlying interaction processes. Track-like events originate mainly from charged-current ν_μ interactions, producing long-range muons that enable precise angular reconstruction. Cascade-like events can result from charged-current ν_e and ν_τ interactions, as well as from neutral-current interactions of all neutrino flavors. These cascades deposit energy in a more spherically distributed pattern, making directional reconstruction inherently more challenging. While track-like events offer superior angular resolution and are ideal for point-source analyses (such as searches for neutrinos from the Sun), cascade-like events provide complementary information through their distinct energy and timing signatures.
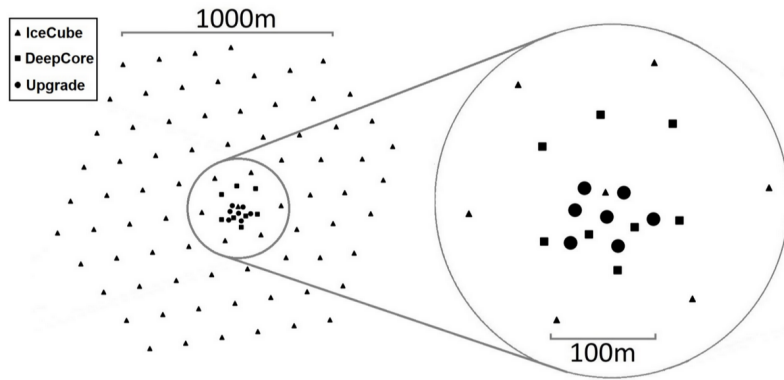
Figure 1: *Top-down View of IceCube Detector.* Each point marks a string of optical modules, with symbols indicating sub-detectors. The enlarged view highlights the denser DeepCore and Upgrade regions.

(a) Effective area

(b) Angular Resolution
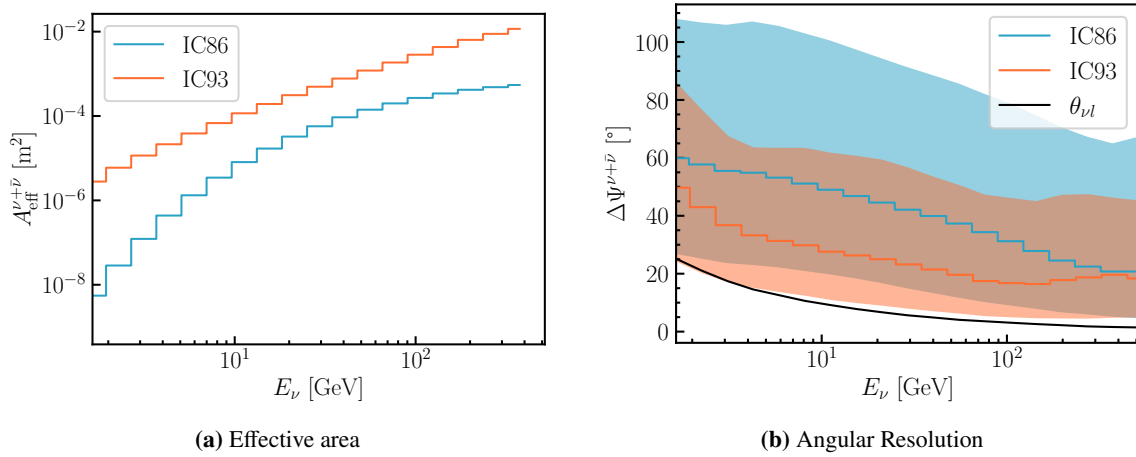
Figure 2: *Detector response comparison between Upgrade and DeepCore.* Left: effective area as a function of neutrino energy. Right: angular resolution (median angle between true and reconstructed direction) as a function of energy; the band shows the 1σ containment region. The black line indicates median angular separation between the neutrino and lepton in charged-current interactions from the simulation dataset processed with an IC93 configuration.

3. Analysis Method

DMs captured in massive bodies like the Sun or Earth through scattering with nuclei can accumulate and eventually annihilate, producing a flux of neutrinos [5]. The time evolution of the number of DMs, $N(t)$, in such a body is governed by:

$$\frac{dN}{dt} = C - C_A N^2 - C_E N,$$

where C is the capture rate and C_A is related to the annihilation cross section and the spatial distribution of DMs within the body and C_E is the evaporation rate. DM evaporation, i.e., re-ejection from the Sun due to rare up-scattering, becomes significant for $m_\chi \lesssim 3.7$ GeV. For larger masses considered in this study this process is negligible [6]. The annihilation rate is therefore given by:

$$\Gamma_A = \frac{1}{2} C_A N^2.$$

Assuming a constant capture rate and no significant evaporation effects, the solution yields the time-dependent annihilation rate:

$$\Gamma_A(t) = \frac{1}{2} C \tanh^2\left(\frac{t}{\tau}\right), \quad \text{where} \quad \tau = \frac{1}{\sqrt{CC_A}}.$$

If the age of the solar system ($t \sim 4.5$ Gyr) is much larger than τ, equilibrium is reached and the annihilation rate simplifies to $\Gamma_A \approx \frac{1}{2}C$, meaning the flux of resulting neutrinos is directly proportional to the capture rate. Importantly this capture rate parameter is proportional to the cross section for DM-proton elastic scattering interaction $\sigma_{\chi p}$. For example for an axial-vector (spin-dependant) interaction between DM and the proton constituting the sun, one can write the following expression for the capture rate:

$$C_{\text{SD}}^\odot = (1.3 \times 10^{25} \text{ s}^{-1}) \, \rho_{0.3} \sigma_{\chi P}^{SD} \frac{S(m_\chi/m_{\text{H}})}{(m_\chi/(1 \text{ GeV}))} \overline{v}_{270},$$

where $\sigma_{\chi P}^{SD}$ is the spin-dependant DM-proton elastic scattering cross section in units of 10^{-40} cm^2, $\overline{v}_{270}$ is the dark matter velocity dispersion in units of 270 km s^{-1}, and $\rho_{0.3}$ is the local halo mass density in units of 0.3 GeV cm^{-3}. $S(m_\chi/m_{\text{H}})$ is the kinematic suppression factor, m_χ is the WIMP mass, and m_{H} is the mass of the hydrogen atom [5]. WIMPs accumulated in the core of the sun can then annihilate into unstable SM particles which themselves could decay into neutrinos. The direct product of the annihilation is called an annhilation channel e.g $\chi\chi \rightarrow b\bar{b}$. Therefore, by searching for neutrinos from the direction of the Sun, IceCube can probe the DM-proton scattering cross section, $\sigma_{\chi p}$, providing complementary and, in some parameter regions, competitive constraints to direct detection experiments.

To perform this analysis, Monte Carlo simulations are used to construct three-dimensional templates for signal and background, binned in reconstructed energy, angular separation from the Sun, and track score—a classifier distinguishing ν_μ charged-current events from other topologies. Signal events are time-sampled within a three-year window starting January 2026, with Sun positions computed using IceCube software interfacing with the Positional Astronomy Library [7]. Events are selected if their true direction lies within the solar disk, considered to have a radius of 695 700 km and
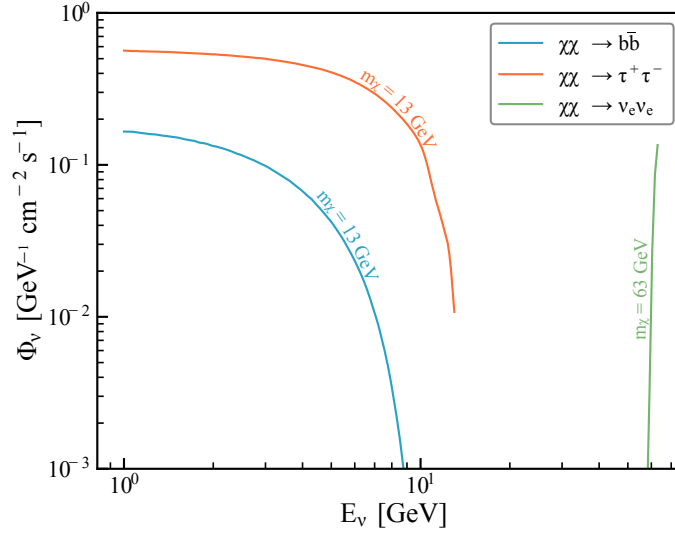
Figure 3: *Neutrino flux for different annihilation channels* The line indicates the neutrino flux at the detector for different initial DM mass and for a nominal $\sigma_{\chi p} = 1 \times 10^{-40} \, \text{cm}^2$

weighted by the product of their MC weight and neutrinos from DM anhilation flux from the χaroν tool [8, 9]. Three representative WIMP annihilation channels are considered: $b\bar{b}$, which produces hadronic final states and results in a soft neutrino energy spectrum; $\tau^+\tau^-$, a leptonic channel yielding a comparatively hard spectrum; and $\nu\bar{\nu}$, which generates a monochromatic neutrino line from two-body decay. The resulting neutrino flux spectra for selected dark matter masses are shown in Fig. 3. This process is repeated to yield a smoothed distribution with a reference cross-section $\sigma_{\chi p} = 1 \times 10^{-40} \, \text{cm}^2$. An example distribution is shown in Fig. 4. As illustrated, events with lower track scores, corresponding to more cascade-like topologies, tend to exhibit poorer angular reconstruction, which is reflected in the broader spread of opening angles to the sun within the distribution. Background contributions in this analysis include atmospheric muons, conventional atmospheric neutrinos, and solar atmospheric neutrinos. The solar atmospheric neutrino template is constructed identically to the signal template, ensuring consistent treatment of solar directional effects. The atmospheric muon and neutrino backgrounds are generated using IC93 simulation datasets, with event rates weighted according to their respective flux models (GaisserH4a + SIBYLL,IPhonda2014) [10–12]. To simulate an isotropic background distribution, each muon and neutrino event is assigned a randomized right ascension uniformly distributed in the range $[0, 2\pi)$, along with a random timestamp sampled within the analysis time window which is then used to calculate the opening angle with the Sun. The total background distribution is obtained by summing all three individual components which is shown in Figure 5.

The sensitivity in this analysis is estimated using trials within a binned Poisson likelihood framework. The likelihood function is defined as:

$$\mathcal{L}(\boldsymbol{\theta} \,|\, \mathbf{n}) = \prod_i \frac{e^{-\mu_i(\boldsymbol{\theta})} \, \mu_i(\boldsymbol{\theta})^{n_i}}{n_i!}, \tag{1}$$

where $\mathbf{n} = \{n_i\}$ denotes the set of observed event counts in each bin i, and $\mu_i(\boldsymbol{\theta})$ is the expected number of events in bin i given the model parameters $\boldsymbol{\theta}$. The parameter vector $\boldsymbol{\theta} = (\alpha_\chi, \alpha_{\text{bg}})$ represents
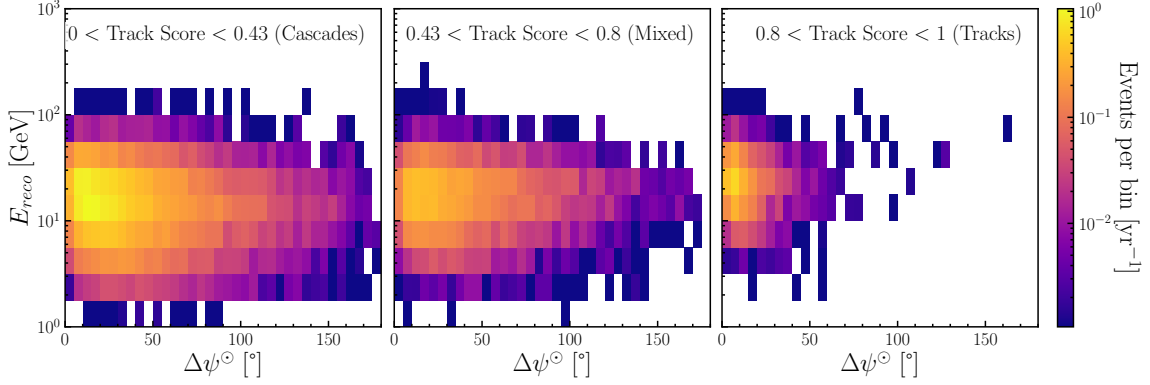
Figure 4: *Example signal distribution for solar DM.* Simulated for DM with mass $m_\chi = 63$ GeV and scattering cross-section $\sigma_{\chi p} = 1 \times 10^{-40}$ cm^2, annihilating to $b\bar{b}$ from the solar core. The distribution is binned in reconstructed energy, angular separation from the Sun, and track score.
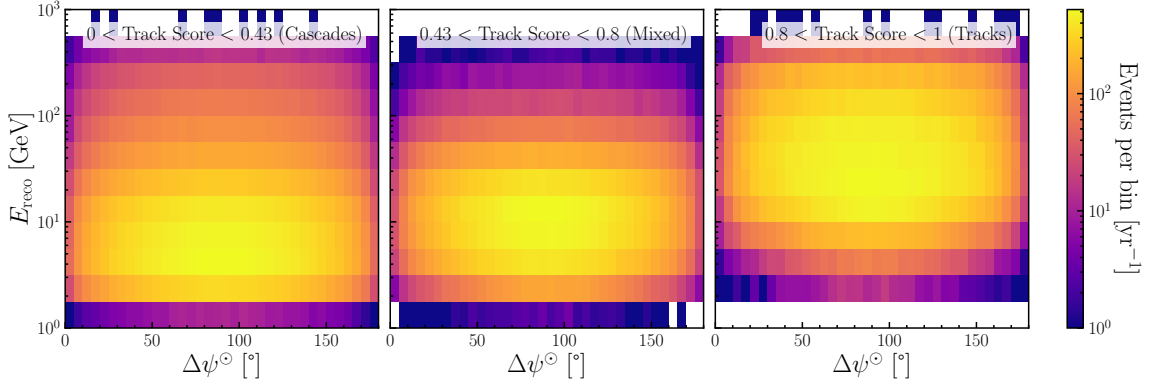
Figure 5: *Background distribution for solar analysis.* Contributions include solar and conventional atmospheric neutrinos and atmospheric muons. Noise events are excluded at final selection level.

the normalization parameters for the potential signal, α_χ (DM-induced solar neutrinos), and for the total background, α_{bg} (including contributions from muons, solar, and conventional atmospheric neutrinos). The expected event count $\mu_i(\boldsymbol{\theta})$ in each bin is modeled as a linear combination of the template distributions:

$$\mu_i(\boldsymbol{\theta}) = \alpha_\chi \, \mu_{\chi,i} + \alpha_{\mathrm{bg}} \, \mu_{\mathrm{bg},i}, \tag{2}$$

where $\mu_{\chi,i}$ denotes the expected number of signal events in bin i, and $\mu_{\mathrm{bg},i}$ denotes the expected number of background events in bin i. The data are binned in $\log_{10}$(reconstructed energy) and in opening angle, with separate bins defined for the track score. This formulation allows the use of binned Poisson statistics to compare the observed data to the model, and evaluate sensitivity by testing different signal strengths α_χ through a hypothesis test. The background test statistic (TS) is defined as:

$$\mathrm{TS}_{\mathrm{bg}} = -2 \left[\log \mathcal{L}(\hat{\alpha}_\chi, \hat{\alpha}_{\mathrm{bg}} \mid \mathbf{n}) - \log \mathcal{L}(\alpha_\chi = 0, \check{\alpha}_{\mathrm{bg}}, \mid \mathbf{n}) \right], \tag{3}$$

where $\check{\alpha}_x$, are best-fit parameters fitting the model including signal from DM anhilation $\theta(\alpha_\chi, \alpha_{bg} = 1)$ onto a data set $\mathbf{n}$ sampled from the background only model $\theta(\alpha_\chi = 0, \alpha_{bg} = 1)$. Due to non-negativity constraints on fit parameters, the TS_{bg} follows a truncated χ^2 distribution with one
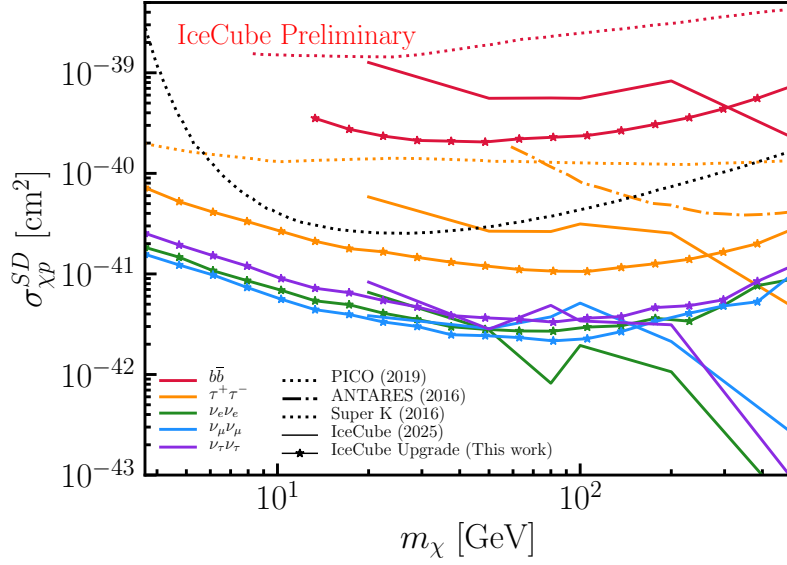
Figure 6: *Sensitivity to DM-proton scattering $\sigma_{\chi p}$ with three years of data.* These projected limits from the IceCube Upgrade would extend IceCube's reach down to 3 GeV, offering complementarity to the lowest masses probed by direct detection experiments. Furthermore, the IceCube Upgrade is expected to deliver world-leading limits on DM-proton scattering cross sections below $O(100)$ GeV. The projected sensitivities are compared to existing limits from [13–15].

degree of freedom: 50% of cases yield TS = 0, and 90% fall below TS_{bg} = 1.64. This threshold is adopted for setting sensitivity targets. Sensitivity is computed as the median signal normalization that results in a TS_{sig} = 1.64 across many trials, providing a robust measure for signal detectability under the given analysis strategy.

$$\text{TS}_{\text{sig}}(\alpha_\chi) = -2 \left[\log \mathcal{L}(\alpha_\chi, \hat{\alpha}_{\text{bg}} \mid \mathbf{n}) - \log \mathcal{L}(\hat{\alpha}_\chi, \hat{\alpha}_{\text{bg}}, \mid \mathbf{n}) \right], \tag{4}$$

4. Results

The sensitivity results, obtained following the methodology in Section 3, are summarized in Fig. 6 and compared with recent results from leading dark matter searches [13–15]. The IceCube Upgrade is projected to achieve the best sensitivity to low-mass DM annihilation up to ~ 210 GeV for the $b\bar{b}$ and $\tau^+\tau^-$ channels, and up to ~ 20 GeV for neutrino final states. The minimum DM mass tested is limited by different factors depending on the channel: for ν and $\tau^+\tau^-$, the constraint arises from the assumption of negligible DM evaporation, valid only above ~ 3.7 GeV [6]; for $b\bar{b}$, it stems from the use of `PYTHIA` in the $\chi a r o \nu$ package, which does not reliably simulate hadronic decays below ~ 10 GeV [16].

5. Conclusion

This work presents a sensitivity study for detecting neutrinos from low-mass dark matter annihilation in the Solar Core using the planned IceCube Upgrade. A dedicated template-based

analysis was developed to search for excess neutrino events from the solar direction, incorporating both track-like and cascade-like topologies. Template construction utilized full MC simulations and flux models for signal and background components, while sensitivity estimates were derived via binned Poisson likelihood pseudo-experiments. The analysis achieves competitive sensitivity projections with three years of data, extending IceCube's reach down to DM masses as low as 3.7 GeV and providing leading limits below $O(100\,\text{GeV})$ for several annihilation channels. The projected performance of the IceCube Upgrade reaffirms its power as a next-generation facility in the search for physics beyond the Standard Model.

References

[1] **SNO Collaboration** Collaboration, Q. R. Ahmad *et al.*, *Phys. Rev. Lett.* **87** (2001) 071301.

[2] M. Schumann, *J. Phys. G* **46** no. 10, (2019) 103003.

[3] **IceCube** Collaboration, M. G. Aartsen *et al.*, *JINST* **12** no. 03, (2017) P03012. [Erratum: JINST 19, E05001 (2024)].

[4] **IceCube** Collaboration, A. Ishihara, *PoS* **ICRC2019** (2021) 1031.

[5] G. Jungman, M. Kamionkowski, and K. Griest, *Physics Reports* **267** no. 5, (1996) 195–373.

[6] A. Gould, *Astrophys. J.* **321** (1987) 560.

[7] T. Jenness and D. S. Berry, "PAL: A Positional Astronomy Library," in *Astronomical Data Analysis*, D. N. Friedel, ed., vol. 475, pp. 307–310. San Francisco, CA, USA, 2013. Available at https://aspbooks.org/publications/475/307.pdf.

[8] Meftah, M., Corbard, T., Hauchecorne, A., Morand, F., Ikhlef, R., Chauvineau, B., Renaud, C., Sarkissian, A., and Damé, L., *AA* **616** (2018) A64.

[9] Q. Liu, J. Lazar, C. A. Argüelles, and A. Kheirandish, *Journal of Cosmology and Astroparticle Physics* **2020** no. 10, (Oct., 2020) 043–043.

[10] T. K. Gaisser, *Astroparticle Physics* **35** (2012) 801–806.

[11] R. S. Fletcher, T. K. Gaisser, P. Lipari, and T. Stanev, *Phys. Rev. D* **50** (1994) 5710–5731.

[12] S. Wren, *Neutrino Mass Ordering Studies with IceCube-DeepCore*. Phd thesis, University of Manchester, 2018.

[13] A.-M. et al., *Physics Letters B* **759** (Aug., 2016) 69–74.

[14] K. Collaboration, "Search for neutrinos from annihilation of captured low-mass dark matter particles in the sun by super-kamiokande," 2015. https://arxiv.org/abs/1503.04858.

[15] C. A. et al., *Physical Review D* **100** no. 2, (Jul, 2019) 022001.

[16] T. Sjöstrand, S. Ask, J. R. Christiansen, R. Corke, N. Desai, P. Ilten, S. Mrenna, S. Prestel, C. O. Rasmussen, and P. Z. Skands, *Computer Physics Communications* **191** (June, 2015) 159–177.

Full Author List: IceCube Collaboration

R. Abbasi[16], M. Ackermann[63], J. Adams[17], S. K. Agarwalla[39, a], J. A. Aguilar[10], M. Ahlers[21], J.M. Alameddine[22], S. Ali[35], N. M. Amin[43], K. Andeen[41], C. Argüelles[13], Y. Ashida[52], S. Athanasiadou[63], S. N. Axani[43], R. Babu[23], X. Bai[49], J. Baines-Holmes[39], A. Balagopal V.[39, 43], S. W. Barwick[29], S. Bash[26], V. Basu[52], R. Bay[6], J. J. Beatty[19, 20], J. Becker Tjus[9, b], P. Behrens[1], J. Beise[61], C. Bellenghi[26], B. Benkel[63], S. BenZvi[51], D. Berley[18], E. Bernardini[47, c], D. Z. Besson[35], E. Blaufuss[18], L. Bloom[58], S. Blot[63], I. Bodo[39], F. Bontempo[30], J. Y. Book Motzkin[13], C. Boscolo Meneguolo[47, c], S. Böser[40], O. Botner[61], J. Böttcher[1], J. Braun[39], B. Brinson[4], Z. Brisson-Tsavoussis[32], R. T. Burley[2], D. Butterfield[39], M. A. Campana[48], K. Carloni[13], J. Carpio[33, 34], S. Chattopadhyay[39, a], N. Chau[10], Z. Chen[55], D. Chirkin[39], S. Choi[52], B. A. Clark[18], A. Coleman[61], P. Coleman[1], G. H. Collin[14], D. A. Coloma Borja[47], A. Connolly[19, 20], J. M. Conrad[14], R. Corley[52], D. F. Cowen[59, 60], C. De Clercq[11], J. J. DeLaunay[59], D. Delgado[13], T. Delmeulle[10], S. Deng[1], P. Desiati[39], K. D. de Vries[11], G. de Wasseige[36], T. DeYoung[23], J. C. Díaz-Vélez[39], S. DiKerby[23], M. Dittmer[42], A. Domi[25], L. Draper[52], L. Dueser[1], D. Durnford[24], K. Dutta[40], M. A. DuVernois[39], T. Ehrhardt[40], L. Eidenschink[26], A. Eimer[25], P. Eller[26], E. Ellinger[62], D. Elsässer[22], R. Engel[30, 31], H. Erpenbeck[39], W. Esmail[42], S. Eulig[13], J. Evans[18], P. A. Evenson[43], K. L. Fan[18], K. Fang[39], K. Farrag[15], A. R. Fazely[5], A. Fedynitch[57], N. Feigl[8], C. Finley[54], L. Fischer[63], D. Fox[59], A. Franckowiak[9], S. Fukami[63], P. Fürst[1], J. Gallagher[38], E. Ganster[1], A. Garcia[13], M. Garcia[43], G. Garg[39, a], E. Genton[13, 36], L. Gerhardt[7], A. Ghadimi[58], C. Glaser[61], T. Glüsenkamp[61], J. G. Gonzalez[43], S. Goswami[33, 34], A. Granados[23], D. Grant[12], S. J. Gray[18], S. Griffin[39], S. Griswold[51], K. M. Groth[21], D. Guevel[39], C. Günther[1], P. Gutjahr[22], C. Ha[53], C. Haack[25], A. Hallgren[61], L. Halve[1], F. Halzen[39], L. Hamacher[1], M. Ha Minh[26], M. Handt[1], K. Hanson[39], J. Hardin[14], A. A. Harnisch[23], P. Hatch[32], A. Haungs[30], J. Häußler[1], K. Helbing[62], J. Hellrung[9], B. Henke[23], L. Hennig[25], F. Henningsen[12], L. Heuermann[1], R. Hewett[17], N. Heyer[61], S. Hickford[62], A. Hidvegi[54], C. Hill[15], G. C. Hill[2], R. Hmaid[15], K. D. Hoffman[18], D. Hooper[39], S. Hori[39], K. Hoshina[39, d], M. Hostert[13], W. Hou[30], T. Huber[30], K. Hultqvist[54], K. Hymon[22, 57], A. Ishihara[15], W. Iwakiri[15], M. Jacquart[21], O. Janik[25], M. Jansson[36], M. Jeong[52], M. Jin[13], N. Kamp[13], D. Kang[30], W. Kang[48], X. Kang[48], A. Kappes[42], L. Kardum[22], T. Karg[63], M. Karl[26], A. Karle[39], A. Katil[24], M. Kauer[39], J. L. Kelley[39], M. Khanal[52], A. Khatee Zathul[39], A. Kheirandish[33, 34], H. Kimku[53], J. Kiryluk[55], C. Klein[25], S. R. Klein[6, 7], Y. Kobayashi[15], A. Kochocki[23], R. Koirala[43], H. Kolanoski[8], T. Kontrimas[26], L. Köpke[40], C. Kopper[25], D. J. Koskinen[21], P. Koundal[43], M. Kowalski[8, 63], T. Kozynets[21], N. Krieger[9], J. Krishnamoorthi[39, a], T. Krishnan[13], K. Kruiswijk[36], E. Krupczak[23], A. Kumar[63], E. Kun[9], N. Kurahashi[48], N. Lad[63], C. Lagunas Gualda[26], L. Lallement Arnaud[10], M. Lamoureux[36], M. J. Larson[18], F. Lauber[62], J. P. Lazar[36], K. Leonard DeHolton[60], A. Leszczyńska[43], J. Liao[4], C. Lin[43], Y. T. Liu[60], M. Liubarska[24], C. Love[48], L. Lu[39], F. Lucarelli[27], W. Luszczak[19, 20], Y. Lyu[6, 7], J. Madsen[39], E. Magnus[11], K. B. M. Mahn[23], Y. Makino[39], E. Manao[26], S. Mancina[47, e], A. Mand[39], I. C. Mariş[10], S. Marka[45], Z. Marka[45], L. Marten[1], I. Martinez-Soler[13], R. Maruyama[44], J. Mauro[36], F. Mayhew[23], F. McNally[37], J. V. Mead[21], K. Meagher[39], S. Mechbal[63], A. Medina[20], M. Meier[15], Y. Merckx[11], L. Merten[9], J. Mitchell[5], L. Molchany[49], T. Montaruli[27], R. W. Moore[24], Y. Morii[15], A. Mosbrugger[25], M. Moulai[39], D. Mousadi[63], E. Moyaux[36], T. Mukherjee[30], R. Naab[63], M. Nakos[39], U. Naumann[62], J. Necker[63], L. Neste[54], M. Neumann[42], H. Niederhausen[23], M. U. Nisa[23], K. Noda[15], A. Noell[1], A. Novikov[43], A. Obertacke Pollmann[15], V. O'Dell[39], A. Olivas[18], R. Orsoe[26], J. Osborn[39], E. O'Sullivan[61], V. Palusova[40], H. Pandya[43], A. Parenti[10], N. Park[32], V. Parrish[23], E. N. Paudel[58], L. Paul[49], C. Pérez de los Heros[61], T. Pernice[63], J. Peterson[39], M. Plum[49], A. Pontén[61], V. Poojyam[58], Y. Popovych[40], M. Prado Rodriguez[39], B. Pries[23], R. Procter-Murphy[18], G. T. Przybylski[7], L. Pyras[52], C. Raab[36], J. Rack-Helleis[40], N. Rad[63], M. Ravn[61], K. Rawlins[3], Z. Rechav[39], A. Rehman[43], I. Reistroffer[49], E. Resconi[26], S. Reusch[63], C. D. Rho[56], W. Rhode[22], L. Ricca[36], B. Riedel[39], A. Rifaie[62], E. J. Roberts[2], S. Robertson[6, 7], M. Rongen[25], A. Rosted[15], C. Rott[52], T. Ruhe[22], L. Ruohan[26], D. Ryckbosch[28], J. Saffer[31], D. Salazar-Gallegos[23], P. Sampathkumar[30], A. Sandrock[62], G. Sanger-Johnson[23], M. Santander[58], S. Sarkar[46], J. Savelberg[1], M. Scarnera[36], P. Schaile[26], M. Schaufel[1], H. Schieler[30], S. Schindler[25], L. Schlickmann[40], B. Schlüter[42], F. Schlüter[10], N. Schmeisser[62], T. Schmidt[18], F. G. Schröder[30, 43], L. Schumacher[25], S. Schwirn[1], S. Sclafani[18], D. Seckel[43], L. Seen[39], M. Seikh[35], S. Seunarine[50], P. A. Sevle Myhr[36], R. Shah[48], S. Shefali[31], N. Shimizu[15], B. Skrzypek[6], R. Snihur[39], J. Soedingrekso[22], A. Søgaard[21], D. Soldin[52], P. Soldin[1], G. Sommani[9], C. Spannfellner[26], G. M. Spiczak[50], C. Spiering[63], J. Stachurska[28], M. Stamatikos[20], T. Stanev[43], T. Stezelberger[7], T. Stürwald[62], T. Stuttard[21], G. W. Sullivan[18], I. Taboada[4], S. Ter-Antonyan[5], A. Terliuk[26], A. Thakuri[49], M. Thiesmeyer[39], W. G. Thompson[13], J. Thwaites[39], S. Tilav[43], K. Tollefson[23], S. Toscano[10], D. Tosi[39], A. Trettin[63], A. K. Upadhyay[39, a], K. Upshaw[5], A. Vaidyanathan[41], N. Valtonen-Mattila[9, 61], J. Valverde[41], J. Vandenbroucke[39], T. van Eeden[63], N. van Eijndhoven[11], L. van Rootselaar[22], J. van Santen[63], F. J. Vara Carbonell[42], F. Varsi[31], M. Venugopal[30], M. Vereecken[36], S. Vergara Carrasco[17], S. Verpoest[43], D. Veske[45], A. Vijai[18], J. Villarreal[14], C. Walck[54], A. Wang[4], E. Warrick[58], C. Weaver[23], P. Weigel[14], A. Weindl[30], J. Weldert[40], A. Y. Wen[13], C. Wendt[39], J. Werthebach[22], M. Weyrauch[30], N. Whitehorn[23], C. H. Wiebusch[1], D. R. Williams[58], L. Witthaus[22], M. Wolf[26], G. Wrede[25], X. W. Xu[5], J. P. Yañez[24], Y. Yao[39], E. Yildizci[39], S. Yoshida[15], R. Young[35], F. Yu[13], S. Yu[52], T. Yuan[39], A. Zegarelli[9], S. Zhang[23], Z. Zhang[55], P. Zhelnin[13], P. Zilberman[39]

1 III. Physikalisches Institut, RWTH Aachen University, D-52056 Aachen, Germany
2 Department of Physics, University of Adelaide, Adelaide, 5005, Australia
3 Dept. of Physics and Astronomy, University of Alaska Anchorage, 3211 Providence Dr., Anchorage, AK 99508, USA
4 School of Physics and Center for Relativistic Astrophysics, Georgia Institute of Technology, Atlanta, GA 30332, USA
5 Dept. of Physics, Southern University, Baton Rouge, LA 70813, USA
6 Dept. of Physics, University of California, Berkeley, CA 94720, USA
7 Lawrence Berkeley National Laboratory, Berkeley, CA 94720, USA
8 Institut für Physik, Humboldt-Universität zu Berlin, D-12489 Berlin, Germany
9 Fakultät für Physik & Astronomie, Ruhr-Universität Bochum, D-44780 Bochum, Germany
10 Université Libre de Bruxelles, Science Faculty CP230, B-1050 Brussels, Belgium

[11] Vrije Universiteit Brussel (VUB), Dienst ELEM, B-1050 Brussels, Belgium

[12] Dept. of Physics, Simon Fraser University, Burnaby, BC V5A 1S6, Canada

[13] Department of Physics and Laboratory for Particle Physics and Cosmology, Harvard University, Cambridge, MA 02138, USA

[14] Dept. of Physics, Massachusetts Institute of Technology, Cambridge, MA 02139, USA

[15] Dept. of Physics and The International Center for Hadron Astrophysics, Chiba University, Chiba 263-8522, Japan

[16] Department of Physics, Loyola University Chicago, Chicago, IL 60660, USA

[17] Dept. of Physics and Astronomy, University of Canterbury, Private Bag 4800, Christchurch, New Zealand

[18] Dept. of Physics, University of Maryland, College Park, MD 20742, USA

[19] Dept. of Astronomy, Ohio State University, Columbus, OH 43210, USA

[20] Dept. of Physics and Center for Cosmology and Astro-Particle Physics, Ohio State University, Columbus, OH 43210, USA

[21] Niels Bohr Institute, University of Copenhagen, DK-2100 Copenhagen, Denmark

[22] Dept. of Physics, TU Dortmund University, D-44221 Dortmund, Germany

[23] Dept. of Physics and Astronomy, Michigan State University, East Lansing, MI 48824, USA

[24] Dept. of Physics, University of Alberta, Edmonton, Alberta, T6G 2E1, Canada

[25] Erlangen Centre for Astroparticle Physics, Friedrich-Alexander-Universität Erlangen-Nürnberg, D-91058 Erlangen, Germany

[26] Physik-department, Technische Universität München, D-85748 Garching, Germany

[27] Département de physique nucléaire et corpusculaire, Université de Genève, CH-1211 Genève, Switzerland

[28] Dept. of Physics and Astronomy, University of Gent, B-9000 Gent, Belgium

[29] Dept. of Physics and Astronomy, University of California, Irvine, CA 92697, USA

[30] Karlsruhe Institute of Technology, Institute for Astroparticle Physics, D-76021 Karlsruhe, Germany

[31] Karlsruhe Institute of Technology, Institute of Experimental Particle Physics, D-76021 Karlsruhe, Germany

[32] Dept. of Physics, Engineering Physics, and Astronomy, Queen's University, Kingston, ON K7L 3N6, Canada

[33] Department of Physics & Astronomy, University of Nevada, Las Vegas, NV 89154, USA

[34] Nevada Center for Astrophysics, University of Nevada, Las Vegas, NV 89154, USA

[35] Dept. of Physics and Astronomy, University of Kansas, Lawrence, KS 66045, USA

[36] Centre for Cosmology, Particle Physics and Phenomenology - CP3, Université catholique de Louvain, Louvain-la-Neuve, Belgium

[37] Department of Physics, Mercer University, Macon, GA 31207-0001, USA

[38] Dept. of Astronomy, University of Wisconsin—Madison, Madison, WI 53706, USA

[39] Dept. of Physics and Wisconsin IceCube Particle Astrophysics Center, University of Wisconsin—Madison, Madison, WI 53706, USA

[40] Institute of Physics, University of Mainz, Staudinger Weg 7, D-55099 Mainz, Germany

[41] Department of Physics, Marquette University, Milwaukee, WI 53201, USA

[42] Institut für Kernphysik, Universität Münster, D-48149 Münster, Germany

[43] Bartol Research Institute and Dept. of Physics and Astronomy, University of Delaware, Newark, DE 19716, USA

[44] Dept. of Physics, Yale University, New Haven, CT 06520, USA

[45] Columbia Astrophysics and Nevis Laboratories, Columbia University, New York, NY 10027, USA

[46] Dept. of Physics, University of Oxford, Parks Road, Oxford OX1 3PU, United Kingdom

[47] Dipartimento di Fisica e Astronomia Galileo Galilei, Università Degli Studi di Padova, I-35122 Padova PD, Italy

[48] Dept. of Physics, Drexel University, 3141 Chestnut Street, Philadelphia, PA 19104, USA

[49] Physics Department, South Dakota School of Mines and Technology, Rapid City, SD 57701, USA

[50] Dept. of Physics, University of Wisconsin, River Falls, WI 54022, USA

[51] Dept. of Physics and Astronomy, University of Rochester, Rochester, NY 14627, USA

[52] Department of Physics and Astronomy, University of Utah, Salt Lake City, UT 84112, USA

[53] Dept. of Physics, Chung-Ang University, Seoul 06974, Republic of Korea

[54] Oskar Klein Centre and Dept. of Physics, Stockholm University, SE-10691 Stockholm, Sweden

[55] Dept. of Physics and Astronomy, Stony Brook University, Stony Brook, NY 11794-3800, USA

[56] Dept. of Physics, Sungkyunkwan University, Suwon 16419, Republic of Korea

[57] Institute of Physics, Academia Sinica, Taipei, 11529, Taiwan

[58] Dept. of Physics and Astronomy, University of Alabama, Tuscaloosa, AL 35487, USA

[59] Dept. of Astronomy and Astrophysics, Pennsylvania State University, University Park, PA 16802, USA

[60] Dept. of Physics, Pennsylvania State University, University Park, PA 16802, USA

[61] Dept. of Physics and Astronomy, Uppsala University, Box 516, SE-75120 Uppsala, Sweden

[62] Dept. of Physics, University of Wuppertal, D-42119 Wuppertal, Germany

[63] Deutsches Elektronen-Synchrotron DESY, Platanenallee 6, D-15738 Zeuthen, Germany

[a] also at Institute of Physics, Sachivalaya Marg, Sainik School Post, Bhubaneswar 751005, India

[b] also at Department of Space, Earth and Environment, Chalmers University of Technology, 412 96 Gothenburg, Sweden

[c] also at INFN Padova, I-35131 Padova, Italy

[d] also at Earthquake Research Institute, University of Tokyo, Bunkyo, Tokyo 113-0032, Japan

[e] now at INFN Padova, I-35131 Padova, Italy

Acknowledgments